water

MDPI

Article

Revealing the Adverse Potential of Six SARS-CoV-2 Antivirals by *Aliivibrio fischeri* Assay: Toxicity Analysis of Single Agent Solutions and Binary Mixtures

Viktorija Martinjak [1], Martina Miloloža [2], Marinko Markić [3,4], Lidija Furač [5], Matija Cvetnić [1], Tomislav Bolanča [1], Dajana Kučić Grgić [2,4] and Šime Ukić [1,*]

[1] Department of Analytical Chemistry, Faculty of Chemical Engineering and Technology, University of Zagreb, Trg Marka Marulića 20, 10000 Zagreb, Croatia; vprevaric@fkit.unizg.hr (V.M.); mcvetnic@fkit.unizg.hr (M.C.); tbolanca@fkit.unizg.hr (T.B.)
[2] Department of Industrial Ecology, Faculty of Chemical Engineering and Technology, University of Zagreb, Trg Marka Marulića 19, 10000 Zagreb, Croatia; miloloza@fkit.unizg.hr (M.M.); dkucic@fkit.unizg.hr (D.K.G.)
[3] Department of Measurements and Process Control, Faculty of Chemical Engineering and Technology, University of Zagreb, Savska cesta 16/5A, 10000 Zagreb, Croatia; mmarkic@fkit.unizg.hr
[4] Comprehensive Water Technology d.o.o., Trg Marka Marulića 19, 10000 Zagreb, Croatia
[5] Department of General and Inorganic Chemistry, Faculty of Chemical Engineering and Technology, University of Zagreb, Trg Marka Marulića 19, 10000 Zagreb, Croatia; lfurac@fkit.unizg.hr
* Correspondence: sukic@fkit.unizg.hr; Tel.: +38-514597217

Abstract: The COVID-19 pandemic has intensified the development of new antiviral agents specifically intended for the SARS-CoV-2 virus, but has also increased the use of some already known antiviral agents originally intended for other viruses. Although the pandemic has ended, the SARS-CoV-2 virus is expected to be present in the human population forever, as is the case with the influenza virus, for example. Such a scenario guarantees the continued use of SARS-CoV-2 antivirals and, accordingly, their continued release into the environment. Unfortunately, there is little or no information on the adverse potential of most of these antiviral agents. In this study, the acute toxicity of six antiviral agents used in the treatment of SARS-CoV-2 infections was determined. These are atazanavir, ribavirin, emtricitabine, nirmatrelvir, sofosbuvir and oseltamivir, sorted according to their toxicity, starting with the most toxic agent. Toxicity was determined using the marine bacterium *Aliivibrio fischeri* according to the ISO 11348-1:2007 standard. In addition to the toxicities of the individual antiviral solutions, the toxicities of binary antiviral mixtures were also determined. By comparing the experimentally determined toxicities of the mixtures with the values estimated by the concentration addition model and the independent action model, we analyzed the mode of joint toxic activity of these antiviral agents. Additive behavior was observed for most binary combinations. The combination of nirmatrelvir and sofosbuvir led to an antagonistic deviation from the concentration addition model, while a synergistic deviation was observed for the combinations of emtricitabine with atazanavir and with nirmatrelvir, as well as for the combinations of ribavirin with atazanavir, oseltamivir and sofosbuvir. All tested binary combinations showed a synergistic deviation from the independent action model.

Keywords: SARS-CoV-2; antivirals; toxicity; mixtures; concentration addition model; independent action model

Citation: Martinjak, V.; Miloloža, M.; Markić, M.; Furač, L.; Cvetnić, M.; Bolanča, T.; Kučić Grgić, D.; Ukić, Š. Revealing the Adverse Potential of Six SARS-CoV-2 Antivirals by *Aliivibrio fischeri* Assay: Toxicity Analysis of Single Agent Solutions and Binary Mixtures. *Water* **2024**, *16*, 3607. https://doi.org/10.3390/w16243607

Academic Editors: Chen Ling and Changqing Zhu

Received: 15 November 2024
Revised: 11 December 2024
Accepted: 12 December 2024
Published: 15 December 2024

1. Introduction

Antimicrobial agents are substances that can kill microorganisms or at least inhibit their growth [1]. Depending on which microorganisms they are intended for, antimicrobials can be classified as antibiotics (bacteria), antifungals (fungi), antiparasitics (parasites) and antivirals (viruses) [2]. In the beginning, people sought and used antimicrobial agents that were available in nature. Over time, however, the discovery of new antimicrobial agents no

longer focused solely on natural sources, but also on the synthesis of new agents which are generally much more selective than the natural ones. Due to the constant need to solve the problems caused by pathogenic microorganisms that are resistant to existing drugs, the pharmaceutical industry is constantly developing new antimicrobial agents [3].

In contrast to antibiotics, which have been developed very intensively and for which there are now numerous drugs to treat a variety of bacterial diseases [4], the development of antifungals, antiparasitics and antivirals has not been as intensive [5–8]. The development of antiviral drugs is a particular challenge [7]. Compared to other pathogens, viruses do not have the usual characteristics of living organisms. They have neither a metabolism nor the ability to self-reproduce. Instead, it is the infected cells that produce new virus individuals. Viruses therefore do not have many proteins or enzymes that could be targeted for treatment [9]. In addition, despite the impossibility of self-reproduction, the reproduction rate of viruses is extremely high, which leads to very rapid mutations [8]. Drugs with a certain degree of effectiveness have already been developed for HIV, herpes, hepatitis, Ebola and various other dangerous viruses [10]. Currently, one of the global priorities is the development of drugs to treat coronavirus infection (COVID-19), an infectious disease caused by the SARS-CoV-2 virus. Although the COVID-19 pandemic (2020–2023) is behind us, humanity has not managed to fully solve the problem of the SARS-CoV-2 virus. It is very likely that people will continue to live with this virus, similar to the coexistence with some other viruses, e.g., the influenza virus.

Scientists are still mainly focused on understanding the mechanisms by which the SARS-CoV-2 virus affects humans and finding new substances that can prevent or at least alleviate the symptoms of the disease. However, there are other aspects related to COVID-19 that also need to be researched in depth. These include the impact of SARS-CoV-2 antiviral agents and their degradation products on the environment [11], as it is known that a certain amount of these substances enters the environment [12]. The human body generally metabolizes 60–70% of active pharmaceutical ingredients, while the remaining unmetabolized substances and metabolites are excreted from the body and thus end up in wastewater [13]. Other possible sources of antivirals in wastewater are hospital waste, wastewater from the pharmaceutical industry and the improper disposal of unused drugs [14]. Unfortunately, it is known that conventional wastewater treatment plants do not remove most pharmaceuticals efficiently [15–17], so they end up in natural receiving waters.

At the beginning of the COVID-19 pandemic, there were neither vaccines nor specific therapeutics for the treatment of COVID-19 infections, so patients were treated with existing drugs intended for infections caused by SARS-CoV-2-like viruses [18]. In the meantime, several new drugs have been developed and put into use [19,20]. However, the analysis of the available literature shows a serious lack of information on the presence, fate and behavior of SARS-CoV-2 antiviral drugs in the environment, whether they are newly developed SARS-CoV-2 drugs or reused drugs originally intended for other viruses, and this information is important to adequately assess the actual risk to the environment.

In this study, we focused on six antiviral substances used to treat COVID-19 infection. These were: atazanavir, emtricitabine, nirmatrelvir, oseltamivir, ribavirin and sofosbuvir. The structures of the selected antivirals are shown in Figure 1 and some basic data are listed in Table 1.

Studies on the environmental concentrations of the six antivirals selected are very rare. Takamami et al. [21] reported a concentration of oseltamivir phosphate of 165.9 ng/L detected in surface water in Japan. Boulard et al. [22] reported an emtricitabine concentration of 0.13 µg/L in effluent of a wastewater treatment plant (WWTP) somewhere in Germany and 0.045 µg/L in nearby surface water. A similar concentration of emtricitabine (0.22 µg/L) was reported by Mlunguza et al. [23] for surface water in the immediate vicinity of the effluent of a WWTP in South Africa. Mhuka et al. [24] analyzed the composition of the effluent of another WWTP in South Africa and found an atazanavir concentration of 75.20 ng/L. All these four reports refer to the time before the COVID-19 pandemic, so it can be assumed that the emergence of the SARS-CoV-2 virus caused an increase in con-

centrations of the aforementioned antiviral agents in aquatic ecosystems. Sometime at the beginning of the COVID-19 pandemic, Chen et al. [25] reported a ribavirin concentration of 52.2 ng/L for rivers in Wuhan Province (China). For the post-pandemic period, we found only two reports: an atazanavir concentration of 0.039 µg/L was detected in water in urban areas of India [26] and an emtricitabine concentration of 358.4 ± 250.8 ng/L was found in drinking water in South Africa [27].

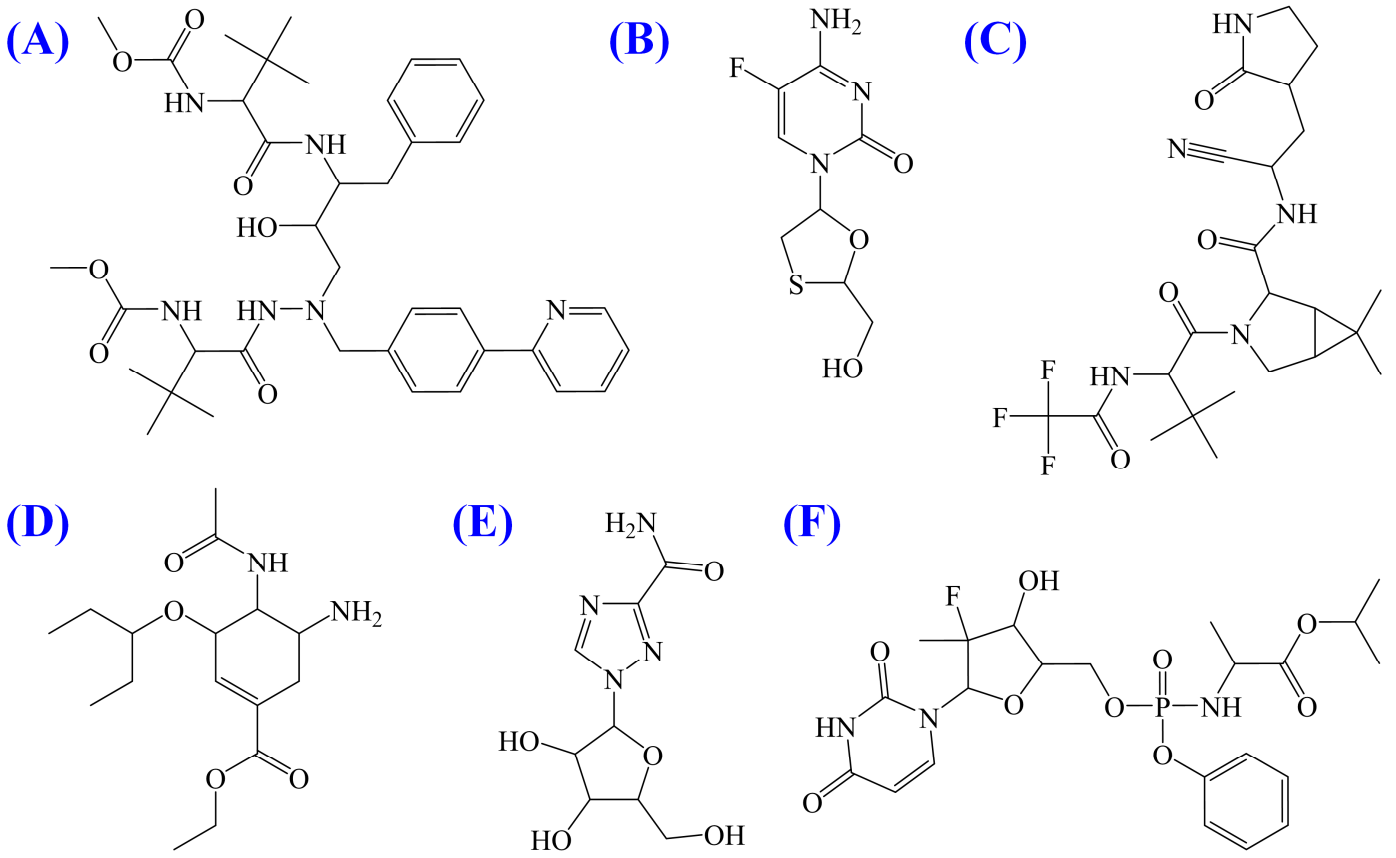

Figure 1. Chemical structures of: (**A**) atazanavir, (**B**) emtricitabine, (**C**) nirmatrelvir, (**D**) oseltamivir, (**E**) ribavirin and (**F**) sofosbuvir.

Table 1. Some basic information on the antiviral agents tested. The logP data were taken from the DrugBank Online database [28].

Antiviral Substance	Molecular Formula	Molar Mass/g mol^{-1}	logP
Atazanavir	$C_{38}H_{52}N_6O_7$	704.86	4.5 *
Emtricitabine	$C_8H_{10}FN_3O_3S$	247.25	−0.43 *
Nirmatrelvir	$C_{23}H_{32}F_3N_5O_4$	499.53	2.12 **
Oseltamivir	$C_{16}H_{28}N_2O_4$	312.40	1 *
Ribavirin	$C_8H_{12}N_4O_5$	244.20	−1.85 *
Sofosbuvir	$C_{22}H_{29}FN_3O_9P$	529.45	1.62 *

Note(s): * Data categorized as experimentally determined; ** data estimated by mathematical model.

Another very important piece of information for environmental risk assessment is information on the toxicity of the substances in question. In this study, the acute toxicity of six selected SARS-CoV-2 antiviral agents was investigated. Acute toxicity was tested on the luminescent marine bacterium *Aliivibrio fischeri*. The toxicity of solutions of pure antiviral substances and of binary antiviral mixtures was analyzed. By applying the concentration addition model and the independent action model, we analyzed the possible synergistic and antagonistic toxic behavior in the antiviral mixtures.

2. Assessment of Toxicity

The term acute toxicity refers to the short-term exposure of organisms to a substance. Acute toxicity is expressed as the effective dose (or effective concentration, *EC*) of a substance, i.e., the dose that causes a certain degree of harm in a tested population of organisms. The toxicity value is assessed mathematically using the so-called dose–response curve, i.e., the relationship between the dose of a substance and the portion of the population affected by that dose. The original sigmoidal form of the dose–response curve is usually linearized by relating the logarithm of the so-called γ-value and the logarithm of the substance dose. The γ-value is defined as the ratio between the affected and the unaffected portion of the tested population. If the percentage of luminescence inhibition (*INH*) is used as an indicator for the affected and unaffected portion of the population, the γ-value can be calculated according to Equation (1):

$$\gamma = \frac{INH}{100 - INH} \quad (1)$$

In most cases, 50% of an adverse effect is used as the threshold for the definition of toxicity. However, in situations where extrapolation is required to determine the dose that produces 50% of the effect in the population, it is better to express toxicity in terms of a lower level of harm (10 or 20%) that allows assessment by interpolation [29].

Various mathematical models have been developed to describe the toxicity of systems containing multiple toxic substances, i.e., toxic mixtures. By comparing the experimentally determined toxicity of the mixture with the toxicity predicted by a mathematical model, possible deviations from the predicted behavior can be identified, be it synergism (the toxicity of the mixture is more pronounced than predicted) or antagonism (the toxicity of the mixture is weaker than predicted).

The concentration addition model [30,31], more simply referred to as the additive model, is the most commonly used model for risk assessment of chemical mixtures [32]. This model is based on the assumption that all toxic substances in the mixture have a common or similar mode of action [33,34]. In its most common form, the additive model uses the so-called toxicity unit (*TU*), which is defined by Equation (2). The numerator of the equation contains the molar concentration (c) of a toxic substance of interest (i) in a mixture that causes the specified level of harm (p) in the population of the test organism. The term in the denominator refers to the toxicity of substance i, expressed as a concentration that causes the same specified level of harm in the tested population [35].

$$TU_i = \frac{c_i}{EC_{p,i}} \quad (2)$$

The independent action model [36] is used much less frequently and, in contrast to the additive model, is based on the assumption that toxic substances in a mixture have different mechanisms of action and therefore have independent toxic effects on the test organism.

3. Materials and Methods

3.1. Reagents and Solutions

Ultrapure water (Millipore) was used for all experiments. Atazanavir sulfate (CAS No. 229975-97-7), emtricitabine (CAS No. 143491-57-0), oseltamivir phosphate (CAS No. 204255-11-8) and ribavirin (CAS No. 36791-04-5), all four manufactured by Supelco (Bellefonte, PA, USA), and nirmatrelvir (CAS No. 2628280-40-8) and sofosbuvir (CAS No. 1190307-88-0), both manufactured by Biosynth (Staad, Switzerland), were used as standards, all in solid form. For each antiviral, a certain amount of the corresponding solid standard was dissolved in water to prepare the stock solution. To improve dissolution, each stock solution was treated with ultrasound. When selecting the values for the stock solutions, we did not rely on data on the concentrations of the tested antiviral drugs in the aquatic environment, as we found that there are almost no studies with such information, especially if we focus on the pandemic and post-pandemic period. All stock solutions were prepared

at a total antiviral concentration of 1.0000 mM, except for the atazanavir solution, which was prepared at a concentration of 0.0030 mM due to the very low solubility of atazanavir sulfate in water. The concentration of the prepared stock solutions was checked by LC analysis. The working solutions of the binary antiviral mixtures were prepared by mixing the solutions of the individual antivirals in the volume ratios 75:25 (MIX 1), 50:50 (MIX 2) and 75:25 (MIX 3).

3.2. Toxicity Experiments

The determination of acute toxicity was carried out on the Gram-negative bacterium *Aliivibrio fischeri* in accordance with ISO 11348-1:2007 [37]. A LUMIStherm thermostat was used to thermostatize the solutions, while the luminescence of the test population of bacteria was measured with a LUMIStox 300 luminometer (both devices are manufactured by Dr. Lange GmbH, Hannover, Germany). The linear sequence of sample dilution was used and the test duration was 30 min.

The bacterial culture used for the toxicity tests was subcultured 24 h before the test on a medium specifically designed to support the growth of *Aliivibrio fischeri*. This step ensured optimal bacterial viability and consistent starting conditions. Prior to testing, the initial luminescence of the bacterial culture was measured and confirmed to be around 3000 relative light units across all tests to ensure comparability of results.

In the toxicity experiments, a 2% NaCl solution in water was used as a control solution. The ratio between the initial and final (30 min) luminescence of the bacteria in the control solutions represented the factor (f) used to correct the initial value of bacterial luminescence in the test solutions (L_0). After measuring the 30 min luminescence of the test solution (L_{30}), the percentage of luminescence inhibition (INH) was calculated according to Equation (3).

$$INH = \frac{L_0 \cdot f - L_{30}}{L_0 \cdot f} \cdot 100 \quad (3)$$

Given the short test duration, all toxicity tests for a specific antiviral compound were performed on the same day. Three technical replicates were performed for each compound to ensure precision and repeatability of measurements; the mean values were used to calculate toxicity. Biological replicates were not included in this study due to the controlled and standardized nature of the experimental conditions and the consistent preparation of the bacterial culture.

3.3. Data Analysis

Experimental data were processed in Excel 2016 software (Microsoft Corporation, Redmond, WA, USA), while toxicity modeling was performed using the MATLAB R2010b software package (The MathWorks Inc., Natick, MA, USA).

4. Results

The first step in this study was to determine the toxicity of the individual antiviral agents. The corresponding dose–response curves are shown in Figure S1. The toxicity values determined are listed in Table 2 together with the parameters of the linear dose–response relationship. The dose–response relationship was linearized to reduce the influence of random errors and to simplify the calculation of EC values. Table 2 shows two toxicity values for each antiviral agent: the one related to 20% inhibition of luminescence (EC_{20}) and the one related to 50% inhibition of luminescence (EC_{50}) in the tested population of *Aliivibrio fischeri*. It should be noted that the toxicity analysis in this study is based on the EC_{20} values, as these values were determined by data interpolation. The 50% inhibition for ribavirin was within the range of experimentally determined inhibitions, but for five other antiviral agents the 50% inhibition was above this range and therefore the corresponding EC_{50} values were estimated by data extrapolation, making the estimated values less reliable. The reason we decided to list these EC_{50} values in Table 2 was that we wanted to have some data to compare with the EC_{50} values that might be found in the literature.

Table 2. Experimentally determined toxicity values according to *Aliivibrio fischeri* test.

Antiviral Substance	Dose–Response Line (log γ = a log c + b)			EC_{20}/ mM (mg L^{-1})	EC_{50}/ mM (mg L^{-1})
	a	b	R^2		
Atazanavir	1.880	4.267	0.9895	0.0026 (1.83)	0.0054 (3.81) *
Emtricitabine	1.654	−0.029	0.9975	0.4504 (111.36)	1.0415 (257.51) *
Nirmatrelvir	2.057	−0.100	0.9968	0.5699 (284.68)	1.1180 (558.47) *
Oseltamivir	2.469	−0.419	0.9980	0.8431 (263.38)	1.4783 (461.82) *
Ribavirin	1.619	0.248	0.9930	0.2986 (72.92)	0.7031 (171.70)
Sofosbuvir	2.317	−0.131	0.9946	0.6260 (331.44)	1.1388 (602.94) *

Note(s): * The value was calculated by data extrapolation.

The next step in this study was to determine the toxicity of antiviral binary mixtures and to analyze their joint toxic activity. The total molar concentration of the antivirals in the binary mixtures tested was 1.0000 mM in most cases; it is easier to compare the mixtures with the same total concentration of antivirals. An exception was the binary mixtures with atazanavir, which were prepared at much lower concentrations due to the poor solubility of atazanavir sulfate (see c_{TOTAL} in Table 3).

Table 3. Regression analysis of dose–response correlation for binary mixtures and the corresponding EC_{20} values. The abbreviations ATA, FTC, NMV, OST, RIB and SOF stand for atazanavir, emtricitabine, nirmatrelvir, oseltamivir, ribavirin and sofosbuvir, respectively.

Binary Combinations					Dose–Response Line (log γ = a log c + b)			EC_{20}/mM
No.	Combination	Mixture	Ratio	c_{TOTAL}/mM	a	b	R^2	
I	ATV–FTC	MIX 1	75:25	0.2522	1.778	0.921	0.9948	0.1392
		MIX 2	50:50	0.5015	1.588	0.390	0.9944	0.2374
		MIX 3	25:75	0.7508	1.736	0.217	0.9937	0.3374
II	ATV–NMV	MIX 1	75:25	0.2522	2.016	0.974	0.9891	0.1652
		MIX 2	50:50	0.5015	1.730	0.276	0.9926	0.3107
		MIX 3	25:75	0.7508	1.962	0.162	0.9879	0.4078
III	ATV–OST	MIX 1	75:25	0.2522	1.998	0.721	0.9945	0.2176
		MIX 2	50:50	0.5015	2.135	0.234	0.9957	0.4061
		MIX 3	25:75	0.7508	2.453	−0.100	0.9894	0.6242
IV	ATV–RIB	MIX 1	75:25	0.2522	1.661	1.030	0.9894	0.1040
		MIX 2	50:50	0.5015	1.672	0.557	0.9939	0.2027
		MIX 3	25:75	0.7508	1.554	0.257	0.9932	0.2802
V	ATV–SOF	MIX 1	75:25	0.2522	1.673	0.673	0.9884	0.1730
		MIX 2	50:50	0.5015	1.847	0.261	0.9914	0.3410
		MIX 3	25:75	0.7508	1.938	0.038	0.9911	0.4674
VI	FTC–NMV	MIX 1	75:25	1.0000	1.807	0.131	0.9963	0.3927
		MIX 2	50:50	1.0000	1.844	0.145	0.9981	0.3935
		MIX 3	25:75	1.0000	1.746	−0.046	0.9929	0.4806
VII	FTC–OST	MIX 1	75:25	1.0000	1.768	−0.038	0.9967	0.4796
		MIX 2	50:50	1.0000	1.704	−0.091	0.9914	0.5012
		MIX 3	25:75	1.0000	2.071	−0.145	0.9939	0.6017
VIII	FTC–RIB	MIX 1	75:25	1.0000	1.720	0.220	0.9960	0.3327
		MIX 2	50:50	1.0000	1.756	0.149	0.9960	0.3733
		MIX 3	25:75	1.0000	1.657	0.115	0.9944	0.3690
IX	FTC–SOF	MIX 1	75:25	1.0000	1.577	−0.061	0.9958	0.4536
		MIX 2	50:50	1.0000	2.250	0.004	0.9967	0.5379
		MIX 3	25:75	1.0000	2.272	−0.044	0.9932	0.5680

Table 3. *Cont.*

Binary Combinations					Dose–Response Line (log $\gamma = a \log c + b$)			EC_{20}/mM
No.	**Combination**	**Mixture**	**Ratio**	c_{TOTAL}/mM	a	b	R^2	
X	NMV–OST	MIX 1	75:25	1.0000	2.078	−0.212	0.9918	0.6489
		MIX 2	50:50	1.0000	2.185	−0.271	0.9959	0.7056
		MIX 3	25:75	1.0000	2.211	−0.324	0.9905	0.7487
XI	NMV–RIB	MIX 1	75:25	1.0000	1.519	0.000	0.9919	0.4015
		MIX 2	50:50	1.0000	1.637	0.061	0.9912	0.3935
		MIX 3	25:75	1.0000	1.718	0.253	0.9932	0.3180
XII	NMV–SOF	MIX 1	75:25	1.0000	2.533	−0.177	0.9941	0.6795
		MIX 2	50:50	1.0000	2.614	−0.231	0.9917	0.7212
		MIX 3	25:75	1.0000	2.504	−0.214	0.9936	0.7000
XIII	OST–RIB	MIX 1	75:25	1.0000	2.039	0.096	0.9908	0.4547
		MIX 2	50:50	1.0000	1.694	0.170	0.9948	0.3501
		MIX 3	25:75	1.0000	1.657	0.248	0.9974	0.3069
XIV	OST–SOF	MIX 1	75:25	1.0000	2.108	−0.428	0.9859	0.8265
		MIX 2	50:50	1.0000	2.282	−0.322	0.9844	0.7534
		MIX 3	25:75	1.0000	2.355	−0.234	0.9889	0.6976
XV	RIB–SOF	MIX 1	75:25	1.0000	1.624	0.272	0.9919	0.2894
		MIX 2	50:50	1.0000	1.637	0.218	0.9912	0.3154
		MIX 3	25:75	1.0000	1.925	0.211	0.9926	0.3780

A regression analysis of the linearized form of the relationship between the antiviral dose (log c) and the response (log γ) was performed for all 45 binary mixtures and relatively high correlations were found ($R^2 \geq 0.9879$; Table 3). The EC_{20} values of the mixtures were calculated by applying the developed regression models. These values and the toxicity values for the individual antivirals were used to calculate the *TU* values according to Equation (2). The isobologram approach, shown in Figure 2, was used to illustrate the deviation from additive behavior. The straight line connecting the points (1, 0) and (0, 1) represents the isobole of the additive behavior of two antiviral agents or simply: the additive isobole. (The isobole is a curve connecting all dose combinations that are expected to produce the same desired response.) *TU* points below the additive isobole indicate possible synergistic behavior of the antiviral agents in their mixture, while *TU* points above this isobole indicate possible antagonism in the antiviral mixture. However, since the determination of toxicity is subject to a certain random error, a prediction band in the range of 0.8–1.2 was defined (the area within the dashed lines).

The results of toxicity prediction by an independent action model are presented for the mixtures of nirmatrelvir and sofosbuvir as well as oseltamivir and sofosbuvir. The results are presented graphically as a comparison between the experimentally determined toxicity values and the values predicted by the model (Figure 3). For comparison purposes, we have also supplemented this graphical presentation with the values predicted by the additive model.

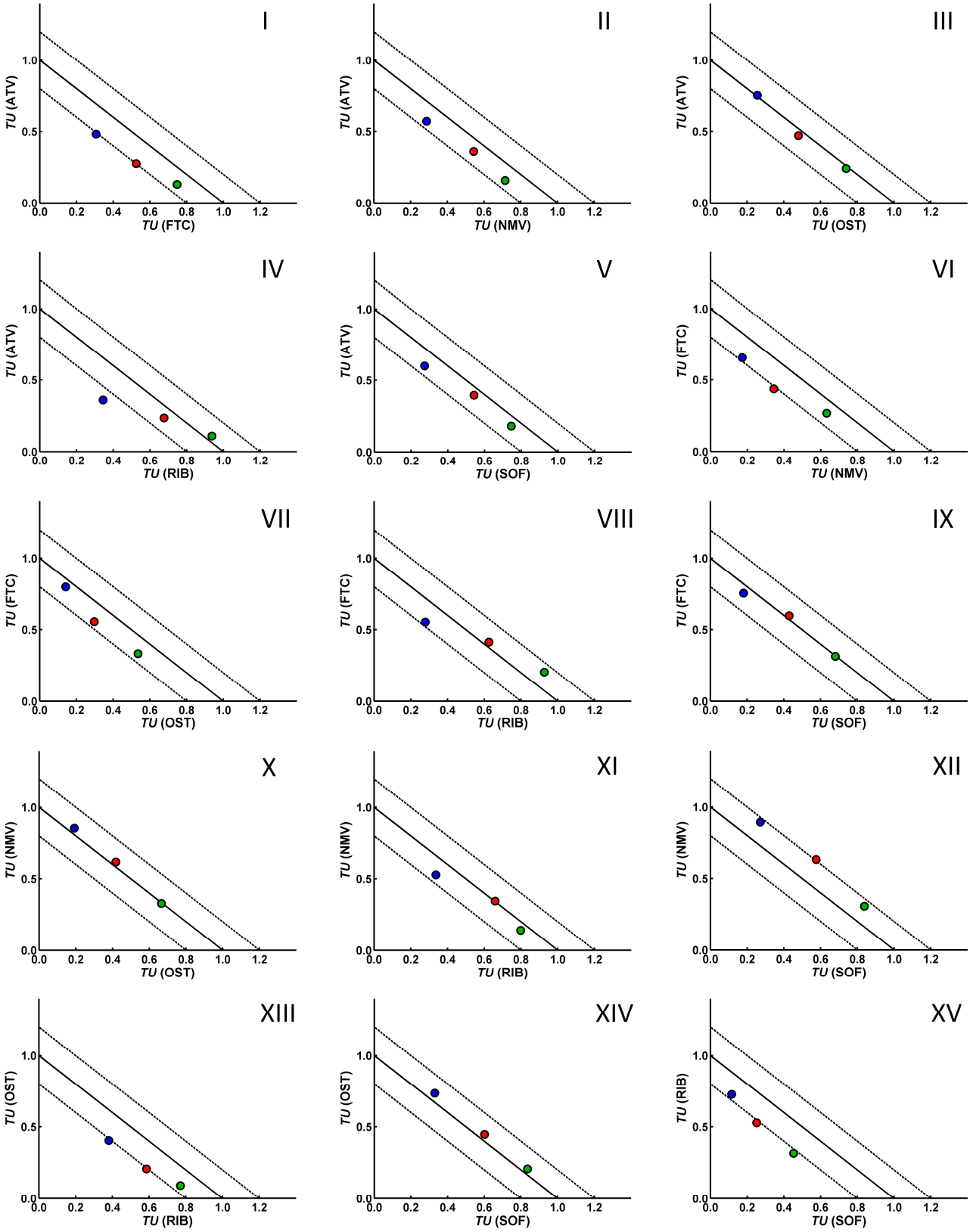

Figure 2. Isobolograms of binary mixtures of antivirals. Comparison of experimentally determined joint toxicity (circles) and additive behavior (solid lines). Different colors represent different binary mixtures, i.e., the mixtures containing different ratios of the individual antiviral solutions: MIX 1 (75:25; blue circle), MIX 2 (50:50, red circle) and MIX 3 (25:75, green circle).

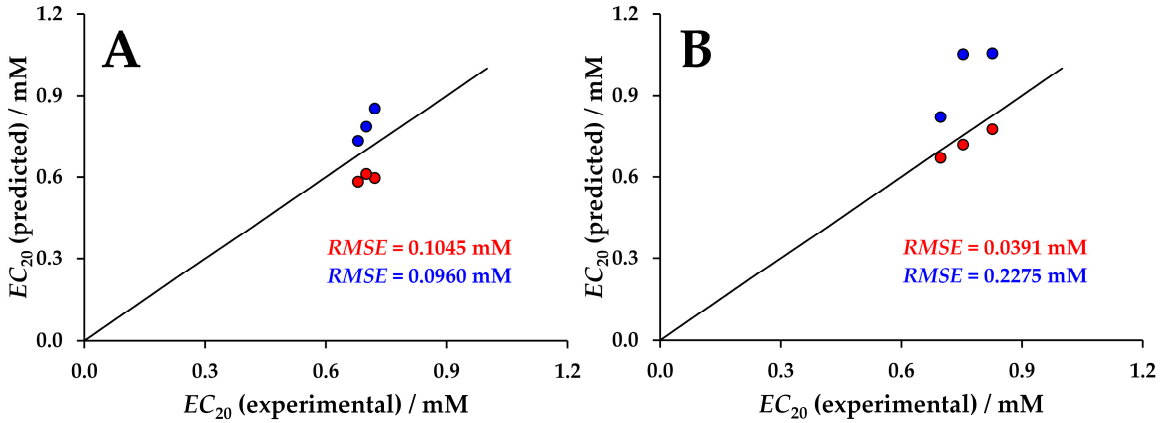

Figure 3. Comparison between the predicted and experimentally determined toxicity values for the mixtures of (**A**) nirmatrelvir and sofosbuvir, and (**B**) oseltamivir and sofosbuvir. The cases correspond to the concentration addition model (red color) and the independent action model (blue color). The straight line is the $y = x$ line, which represents the ideal scenario where the predicted values agree with the experimentally obtained values.

5. Discussion

The aim of our study was to reveal the adverse potential of selected antiviral agents and their mixtures in the aquatic environment. For this purpose, we performed the *Aliivibrio fischeri* bioluminescence inhibition assay. Performing bioassays with different types of organisms (plants, algae, daphnids, fish and crustaceans) can provide additional information, as different organisms may respond to different antiviral concentrations. However, bioassays with multicellular organisms are associated with high costs and a long test duration, which is not the case for bioassays based on bacterial cells such as the applied *Aliivibrio fischeri* assay. In addition, the *Aliivibrio fischeri* assay is mostly more sensitive than conventional bioassays based on plants, algae, daphnids, fish and crustaceans and has a relatively high reliability and reproducibility [38].

In reviewing the literature, we found some studies in which bioassays were performed with the same or similar organisms, but not for all six of the antivirals we tested. Wherever possible, we have discussed this information in the context of our results. We have not discussed the toxicity results obtained by assays with significantly different organisms, such as eukaryotes, as we recognize that the sensitivity of such organisms is likely to be significantly different from that of *Aliivibrio fischeri*.

Our results of the *Aliivibrio fischeri* assay show that atazanavir is by far the most toxic of the antivirals tested (Table 2): it is two orders of magnitude more toxic than the others. Atazanavir is followed by ribavirin, emtricitabine, nirmatrelvir, sofosbuvir and the least toxic oseltamivir. The mechanisms of action of the tested antiviral agents on *Aliivibrio fischeri* were not examined in this study, only the extent of the effect. Therefore, the reason for this order of toxicity can only be speculated, considering that the toxicity of each substance depends on its molecular structure. For example, many aromatic hydrocarbons are considered to be a considerable hazard to living organisms [39,40]. So, if the main cause of toxicity of these two antiviral agents is their aromatic nature, then it is not surprising that atazanavir, which contains three aryl groups, is much more toxic than sofosbuvir, which contains only one aryl group. Emtricitabine, the next in the series of selected antiviral agents, is a derivative of 1,3-oxathiolane and these derivatives are known for their antimicrobial properties [41]. The structure of nirmatrelvir contains a nitrile group, which in principle does not pose a serious toxic risk as long as this group is incorporated into the organic structure. However, it is very likely that highly toxic cyanide ions or HCN are formed during the degradation of nirmatrelvir, which can definitely increase the toxicity of the antiviral solution. In the case of oseltamivir, we cannot identify a specific group in the molecular structure that we suspect as a possible cause of the toxicity of this antiviral

agent. However, oseltamivir is a so-called prodrug [42], i.e., a substance that has little or no pharmacological activity until it is metabolized to more active compounds [43]. We found two literature reports on the toxicity of oseltamivir to *Aliivibrio fischeri*. In the first report, Escher at al. [44] give an EC_{50} value of 10 mM, which is about 10 times higher than the value we calculated by data extrapolation. The study by van Beek [45] provides less comparable information, as the author performed a 5 min toxicity experiment exposing *Aliivibrio fischeri* to a 1 µM solution of oseltamivir; accordingly, he did not report an EC_{50} value, but only that the applied oseltamivir concentration did not cause luminescence inhibition. Ribavirin contains a 1,2,4-triazole ring in its structure, which can impair lipid metabolism and energy production [46]. In addition, ribavirin is a derivative of furan, which is known to be a very toxic substance: the EC_{15} value for furan according to the *Aliivibrio fischeri* test (15 min exposure) was reported to be 0.05794 mM [47]. Unfortunately, we could not find comparable toxicity data for ribavirin in the literature. Guo et al. [48] tested the toxicity of ribavirin on the bacterium *Photobacterium phosphoreum*, which, like *Aliivibrio fischeri*, is a luminescent Gram-negative marine bacterium. They found no inhibition of luminescence during a 15 min exposure to a 0.1 mM ribavirin solution. Finally, Kalyaev et al. [49] tested the toxicity of some other furan derivatives and reported their antimicrobial activity against fungi and bacteria. Sofosbuvir, the latest in a series of antiviral drugs selected in this study, is by nature a phosphonate, namely a phosphoramidate. Many phosphoramidates are used as insecticides [50], which means that they have biocidal potential. Like oseltamivir, sofosbuvir is designed as a prodrug and should therefore become more active during metabolic transformation within the bacterial cell. It is assumed that the enzymes esterase, hydrolase and phosphoramidase are required for the activation of sofosbuvir [51]. *Aliivibrio fischeri* is known to be able to produce all of these enzymes [52,53], which opens up the possibility of enhancing the toxic effect of sofosbuvir through metabolic activation.

Considering the physicochemical properties of the tested antivirals, we decided to relate the obtained toxicities (Table 2) to the hydrophobicity of the tested antivirals, in particular to the logarithmic value of the octanol–water partition coefficient (logP; Table 1), since there are reports [54,55] that the acute toxicity of some organic molecules to *Aliivibrio fischeri* correlates linearly with the logP value. Here, we encountered the problem that there was a lack of reliable literature data on the logP values of selected antiviral agents. We did not find any scientific reports in which these logP values were determined experimentally. LogP values can be found in various databases accessible via the Internet, most of which offer values estimated using mathematical models. For the logP values listed in these databases as experimentally determined, the references from which they were taken are often not given or they do not provide clear evidence that the values given were actually experimentally determined. We decided to use the logP data from the DrugBank Online [28] database (https://go.drugbank.com (accessed on 9 October 2024), version 5.1.12). In addition to the experimentally determined logP values (which also suffer from the above-mentioned unreliability of the data source), the DrugBank Online database also provides values predicted by the ALOGPS software 2.1 [56]. The database contains experimental values for all tested antivirals except nirmatrelvir. However, since a relative agreement between the experimental logP values and the values estimated by the software was observed for the other five antivirals, we assume that the estimated value for nirmatrelvir should also not differ significantly from the actual value. The typical range of logP values of organic substances ranges from –3 for very hydrophilic to 10 for extremely hydrophobic substances [57], with positive logP values indicating a certain hydrophobic character of the substance [58]. It can therefore be seen (Table 1) that four of the selected antiviral substances, namely atazanavir, nirmatrelvir, oseltamivir and sofosbuvir, have a pronounced hydrophobic character to a certain degree, while emtricitabine and ribavirin can be regarded as highly hydrophilic. The regression analysis between the toxicity and the logP value of the six tested antivirals showed no linear correlation (R^2 value was 0.0815). However, when two highly hydrophilic antivirals, emtricitabine and ribavirin, were excluded from the analysis, a high linear correlation (R^2 of 0.9921) was observed (Figure 4A). This suggests

a possible similarity in the nature of the toxic action of atazanavir, nirmatrelvir, sofosbuvir and oseltamivir. Accordingly, it also implies that the mode of action of emtricitabine and ribavirin probably differs substantially from that of the other four antivirals.

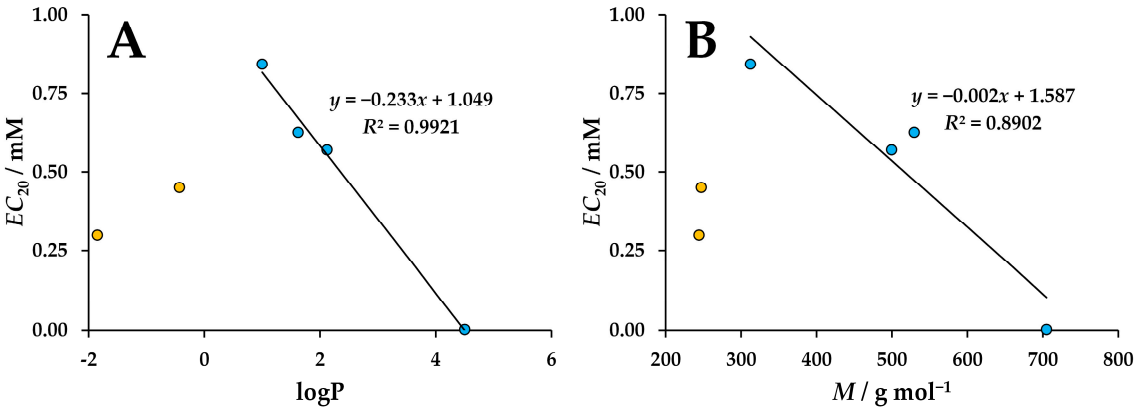

Figure 4. Correlation between toxicity and (**A**) the logP value, and (**B**) molar mass, for atazanavir, nirmatrelvir, oseltamivir and sofosbuvir (blue circles). The orange circles represent the highly hydrophilic antiviral agents emtricitabine and ribavirin, which were excluded from the regression analysis.

The cell membrane is constructed as a phospholipid bilayer, with the hydrophilic head of each phospholipid facing outwards, while the hydrophobic tails of the phospholipids are contained within the membrane [59]. In this way, the outer part of the cell membrane is hydrophilic, while the inner part is hydrophobic. Some scientists are of the opinion that with such a construction of the cell membrane, substances with high logP values can accumulate in the cell membrane due to the preferential interaction with the inner hydrophobic part of the membrane and thus have an adverse effect [54]. It is clear that with this type of toxic action, the increase in molecule size leads to higher toxicity. We therefore correlated the molar mass of the antivirals, which we took as a measure of the size of the molecule, with the toxicity values (Figure 4B) and again found a relatively high linearity (R^2 of 0.8902); of course, this did not apply to emtricitabine and ribavirin.

An important part of this study was the analysis of the joint toxic activity of selected antiviral agents, of course taking into account the results of toxic activity against the bacterial culture *Aliivibrio fischeri*. After a thorough analysis of the literature, we found no studies addressing the joint ecotoxicological activity of selected antiviral agents. Of course, it is possible to find some information on the joint activity against viruses, but this information is not too comparable with the antibacterial activity investigated in this study, considering that viruses do not have the usual characteristics of living organisms and that a significant difference in the mechanisms of action is to be expected.

The isobolographic analysis for most of the binary combinations showed that the joint toxic effect of the antiviral agents follows an additive behavior (Figure 2, cases II, III, V, VII–X, XII and XIV). A synergistic deviation from additivity was observed in some combinations containing emtricitabine or ribavirin, which supports our earlier observation coming form Figure 4 that emtricitabine and ribavirin may have different toxic modes of action compared to the other four antivirals. Thus, the combination of emtricitabine and atazanavir (Figure 2, case I) clearly shows a synergistic effect at higher concentrations of atazanavir, while the *TU* point of the mixture with the lowest concentration of atazanavir is in the additivity range. The behavior in which the *TU* point of a mixture approaches the additive isobole as the composition of the mixture approaches the composition of a single-antiviral solution is logical, since the influence of a high concentration of one antiviral masks the influence of the other antiviral. The combination of emtricitabine and nirmatrelvir (Figure 2, case VI) shows a similar trend in behavior, but only the *TU* point related to MIX 2 (red circle) is below the additivity prediction band, while the other two *TU* points are within the band. The combination of emtricitabine and oseltamivir (Figure 2, case

VII) also tends towards synergism, but none of the three *TU* points lie outside the additivity prediction band, so we cannot be sure whether it is synergism or whether the position of the *TU* points was actually influenced by random error. An interesting situation was observed with the combination of emtricitabine and ribavirin (Figure 2, case VIII). Although all three *TU* points are within the additivity prediction band, indicating an additive behavior of the antiviral agents, the distribution of the points is very interesting. In the mixture with a high portion of emtricitabine (MIX 1), the *TU* point is close to the lower edge of the additivity prediction band. In mixtures with equal portions of emtricitabine and ribavirin (MIX 2), the *TU* point lies along the additivity line, whereas with high portions of ribavirin (MIX 3) it lies closer to the upper edge of the additivity prediction band. This type of behavior suggests that the mask of additivity maybe conceal a dose-dependent switch between synergism and antagonism that was not fully expressed in the selected experiments. It should be noted that the alternation between synergistic and antagonistic effects depending on the dose of the respective antiviral is not uncommon for SAR-CoV-2 designated antivirals [60]. In binary mixtures containing ribavirin, synergism is observed when ribavirin is combined with atazanavir (Figure 2, case IV), oseltamivir (Figure 2, case XIII) and sofosbuvir (Figure 2, case XV). In the case of the combination with atazanavir (Figure 2, case IV), the mixture with 75% of the atazanavir solution (MIX 1) clearly shows a synergistic behavior; however, the behavior becomes additive with lower portions of atazanavir (MIX 2 and MIX 3). When ribavirin is combined with oseltamivir (Figure 2, case XIII), synergism is slightly masked at low ribavirin concentrations. A similar masking of synergism is observed at high ribavirin concentrations when ribavirin is combined with sofosbuvir (Figure 2, case XV).

The combination of nirmatrelvir and sofosbuvir (Figure 2, case XII) and that of oseltamivir and sofosbivir (Figure 2, case IV) were the only combinations that resulted in *TU* points that deviated antagonistically from the additive isobole. However, the combination of nirmatrelvir and sofosbuvir is the only combination that we can truly associate with antagonism, as all three *TU* points lie near the upper edge of the additivity prediction band, with the point relating to MIX 2 lying outside the additivity prediction band. In the case of the combination of oseltamivir and sofosbuvir, all *TU* points are within the additivity prediction band. Moreover, they are relatively close to the additive isobole, indicating that the nature of the joint toxic activity of these two antivirals is indeed additive.

It is known that the independent action model always predicts a lower toxicity of a mixture (i.e., higher EC values) than the concentration addition model [29]. Therefore, independence in the toxic action of two antivirals can only be expected for binary combinations that exhibit antagonistic deviation from the additive isobole. Accordingly, we applied the independent action model to only two of the previously discussed combinations: the combination of nirmatrelvir and sofosbuvir (Figure 2, case XII) and that of oseltamivir and sofosbivir (Figure 2, case XIV). The toxicity values predicted by the independent action model were compared with the experimentally obtained values (Figure 3). We also supplemented Figure 3 with data predicted by the concentration addition model to see whether or not the independent mode of action dominates over the additive behavior of the antivirals.

Figure 3A, which presents the data for the combination of nirmatrelvir and sofosbuvir, shows a very similar extent of deviation of the data points from the $y = x$ line for both toxicity models, with a visible antagonistic deviation from the additivity model and a synergistic deviation from the independent action model. The root mean squared error (*RMSE*) value of 0.0960 mM indicates a relatively high degree of independence in the toxic action of these two antivirals. Although this value is slightly lower than the *RMSE* value obtained for the additive model, which speaks for the better applicability of the independent action model, the fact that the determination of toxicity is subject to some random error should not be forgotten. Therefore, it does not seem justified to consider a difference of only 0.0085 mM as conclusive evidence that the joint toxic effect of these two antivirals is primarily due to independence of action. A more realistic scenario seems to be that the toxicity of these two antivirals results from multiple mechanisms of action, some of which contribute to additivity and some of which are independent. Figure 3B,

corresponding to the combination of oseltamivir and sofosbuvir, confirms that the observed slight antagonistic deviation from the additive isobole is not due to the independence of the toxic action of these antivirals, as the RMSE value for the additive model is significantly lower than that for the independent action model. This supports our earlier observation that the joint toxic action of oseltamivir and sofosbuvir is indeed additive.

6. Conclusions

This study investigated the acute toxicity of six SARS-CoV-2 antivirals and their binary mixtures. The bacterium *Aliivibrio fischeri* was used as the test organism. To avoid toxicity assessment by extrapolation of the experimental data, we chose a 20% inhibition of luminescence of the tested bacterial population as the threshold for the definition of toxicity.

Among the tested antivirals, atazanavir proved to be by far the most toxic (two orders of magnitude more toxic than the others), followed by ribavirin, emtricitabine, nirmatrelvir, sofosbuvir and oseltamivir. Although the mechanisms of toxic action were not investigated in this study, we found that the toxicity of the antivirals with a pronounced hydrophobic character (atazanavir, nirmatrelvir, oseltamivir and sofosbuvir) is strongly dependent on the logP value and the size of the molecule. This could be a good starting point for determining the mechanisms of their toxic action on *Aliivibrio fischeri* and other non-viral organisms.

The analysis of the toxicity of binary combinations of antivirals was performed with the aim of confirming the mode of joint toxic action of the selected antivirals, using the additive model and the independent action model. Most of the binary combinations studied showed additive behavior. In some of the binary combinations containing emtricitabine or ribavirin, a synergistic deviation from the additive model and thus also from the independent action model was observed. These were combinations of emtricitabine with atazanavir and nirmatrelvir as well as combinations of ribavirin with atazanavir, oseltamivir and sofosbuvir. The combination of nirmatrelvir and sofosbuvir was the only combination that showed an antagonistic deviation from the additive model. The use of the independent action model for this combination resulted in a better agreement with the experimentally determined toxicities compared to those obtained with the additive model. Nevertheless, the superiority of the prediction does not appear to be sufficiently better to claim that the joint toxic effect of these two antiviral agents is dominated by the independent mode of action.

Given the study conducted, it is evident that SARS-CoV-2 antivirals and their mixtures have a pronounced adverse potential that should not be ignored. It would therefore be desirable to carry out additional studies that include toxicity analyzes on other organisms (plants, algae, daphnids, fish and crustaceans), but also to determine the actual concentrations of these antivirals in the environment. In addition, the fate of these antivirals in the environment must be investigated, taking into account that the degradation (by)products are often more toxic than the original substances. On this basis, it would be possible to carry out a comprehensive assessment of the environmental risk.

Supplementary Materials: The following supporting information can be downloaded at: https://www.mdpi.com/article/10.3390/w16243607/s1, Figure S1: Dose-response curves to determine the acute toxicity of: (A) atazanavir, (B) emtricitabine, (C) nirmatrelvir, (D) oseltamivir, (E) ribavirin, and (F) sofosbuvir, against the bacterium *Aliivibrio fischeri*. The cases marked with the numbers 1 and 2 indicate the non-linearized and linearized form of the dose-response relationship, respectively.

Author Contributions: Conceptualization, V.M., D.K.G. and Š.U.; methodology, V.M., M.M. (Martina Miloloža), M.M. (Marinko Markić), L.F. and M.C.; formal analysis, V.M.; writing—original draft preparation, V.M. and Š.U.; writing—review and editing, D.K.G., M.C. and Š.U; visualization, V.M. and Š.U; supervision, T.B.; project administration, Š.U. All authors have read and agreed to the published version of the manuscript.

Funding: The authors would like to acknowledge the financial support of the Croatian Science Foundation through the project Environmental Aspects of SARS-CoV-2 Antiviral Substances (EnA-SARS; IP-2022-10-2822).

Data Availability Statement: Data are contained within the article.

Conflicts of Interest: Authors Marinko Markić and Dajana Kučić Grgić are affiliated to the company Comprehensive Water Technology d.o.o. The remaining authors declare that the research was conducted in the absence of any commercial or financial relationships that could be construed as a potential conflict of interest.

References

1. Burnett-Boothroyd, S.C.; McCarthy, B.J. 13—Antimicrobial treatments of textiles for hygiene and infection control applications: An industrial perspective. In *Textiles for Hygiene and Infection Control*; McCarthy, B.J., Ed.; Woodhead Publishing: Oxford, UK, 2011; pp. 196–209. [CrossRef]
2. World Health Organization. Antimicrobial Resistance. Available online: https://www.who.int/news-room/fact-sheets/detail/antimicrobial-resistance (accessed on 24 May 2024).
3. Duval, R.E.; Grare, M.; Demoré, B. Fight Against Antimicrobial Resistance: We Always Need New Antibacterials but for Right Bacteria. *Molecules* **2019**, *24*, 3152. [CrossRef]
4. Hutchings, M.I.; Truman, A.W.; Wilkinson, B. Antibiotics: Past, present and future. *Curr. Opin. Microbiol.* **2019**, *51*, 72–80. [CrossRef]
5. Roemer, T.; Krysan, D.J. Antifungal Drug Development: Challenges, Unmet Clinical Needs, and New Approaches. *Cold Spring Harb. Perspect. Med.* **2014**, *4*, a019703. [CrossRef]
6. Woods, D.J.; Williams, T.M. The challenges of developing novel antiparasitic drugs. *Invertebr. Neurosci.* **2007**, *7*, 245–250. [CrossRef]
7. Bryan-Marrugo, O.L.; Ramos-Jiménez, J.; Barrera-Saldaña, H.; Rojas-Martínez, A.; Vidaltamayo, R.; Rivas-Estilla, A.M. History and progress of antiviral drugs: From acyclovir to direct-acting antiviral agents (DAAs) for Hepatitis C. *Med. Univ.* **2015**, *17*, 165–174. [CrossRef]
8. Howes, L. Why are antivirals so hard to develop? *Chem. Eng. News* **2021**, *99*, 32–35. [CrossRef]
9. Chow, D. Why Are Viruses Hard to Kill? Virologists Explain Why These Tiny Parasites Are so Tough to Treat. Available online: https://www.nbcnews.com/science/science-news/why-are-viruses-hard-kill-virologists-explain-why-these-tiny-n1202046 (accessed on 24 May 2024).
10. De Clercq, E.; Li, G. Approved antiviral drugs over the past 50 years. *Clin. Microbiol. Rev.* **2016**, *29*, 695–747. [CrossRef]
11. Race, M.; Ferraro, A.; Galdiero, E.; Guida, M.; Núñez-Delgado, A.; Pirozzi, F.; Siciliano, A.; Fabbricino, M. Current emerging SARS-CoV-2 pandemic: Potential direct/indirect negative impacts of virus persistence and related therapeutic drugs on the aquatic compartments. *Environ. Res.* **2020**, *188*, 109808. [CrossRef]
12. Gwenzi, W.; Selvasembian, R.; Offiong, N.-A.O.; El Din Mahmud, A.; Sanganyado, E.; Mal, J. COVID-19 drugs in aquatic systems: A review. *Environ. Chem. Lett.* **2022**, *20*, 1275–1294. [CrossRef] [PubMed]
13. Moratalla, A.; Cotillas, S.; Lacasa, E.; Cañizares, P.; Rodrigo, M.A.; Sáez, C. Electrochemical technologies to decrease the chemical risk of hospital wastewater and urine. *Molecules* **2021**, *26*, 6813. [CrossRef]
14. Jain, S.; Kumar, P.; Vyas, R.K.; Pandit, P.; Dalai, A.K. Occurrence and Removal of Antiviral Drugs in Environment: A Review. *Water Air Soil Pollut.* **2013**, *224*, 1410. [CrossRef]
15. Periša, M.; Babić, S. Farmaceutici u okolišu. *Kem. Ind.* **2016**, *65*, 471–482. [CrossRef]
16. Papac Zjačić, J.; Morović, S.; Košutić, K.; Ašperger, D. Combined Application of Membrane and Advanced Oxidation Processes for Removal of Pharmaceuticals from Water. *Kem. Ind.* **2022**, *71*, 719–727. [CrossRef]
17. Kuroda, K.; Li, C.; Dhangar, K.; Kumar, M. Predicted occurrence, ecotoxicological risk and environmentally acquired resistance of antiviral drugs associated with COVID-19 in environmental waters. *Sci. Total Environ.* **2021**, *776*, 145740. [CrossRef] [PubMed]
18. Castañeda-Juárez, M.; Linares-Hernández, I.; Martínez-Miranda, V.; Teutli-Sequeira, E.A.; Castillo-Suárez, L.A.; Sierra-Sánche, A.G. SARS-CoV-2 pharmaceutical drugs: A critical review on the environmental impacts, chemical characteristics, and behavior of advanced oxidation processes in water. *Environ. Sci. Pollut. Res.* **2022**, *29*, 67604–67640. [CrossRef]
19. Treatments for COVID-19. Available online: https://www.nhs.uk/conditions/coronavirus-covid-19/self-care-and-treatments-for-coronavirus/treatments-for-coronavirus/ (accessed on 24 May 2024).
20. Katella, K. COVID-19 Treatments: What We Know So Far. Available online: https://www.yalemedicine.org/news/covid-19-treatment-drugs (accessed on 24 May 2024).
21. Takamami, R.; Ozaki, H.; Giri, R.R.; Taniguchi, S.; Hayashi, S. Antiviral drugs zanamivir and oseltamivir found in wastewater and surface water in Osaka, Japan. *J. Water Environ. Technol.* **2012**, *10*, 57–68. [CrossRef]
22. Boulard, L.; Dierkes, G.; Ternes, T. Utilization of large volume zwitterionic hydrophilic interaction liquid chromatography for the analysis of polar pharmaceuticals in aqueous environmental samples: Benefits and limitations. *J. Chrom. A* **2018**, *1535*, 27–43. [CrossRef] [PubMed]
23. Mlunguza, N.Y.; Ncube, S.; Mahlambi, P.N.; Chimuka, L.; Madikizela, L.M. Determination of selected antiretroviral drugs in wastewater, surface water and aquatic plants using hollow fibre liquid phase microextraction and liquid chromatography-tandem mass spectrometry. *J. Hazard. Mater.* **2020**, *382*, 121067. [CrossRef]

24. Mhuka, V.; Dube, S.; Nindi, M.M. Occurrence of pharmaceutical and personal care products (PPCPs) in wastewater and receiving waters in South Africa using LC-Orbitrap^{TM} MS. *Emerg. Contam.* **2020**, *6*, 250–258. [CrossRef]
25. Chen, X.; Lei, L.; Liu, S.; Han, J.; Li, R.; Men, J.; Li, L.; Wei, L.; Sheng, Y.; Yang, L.; et al. Occurrence and risk assessment of pharmaceuticals and personal care products (PPCPs) against COVID-19 in lakes and WWTP-river-estuary system in Wuhan, China. *Sci. Total Environ.* **2021**, *792*, 148352. [CrossRef]
26. Brauns, B.; Chandra, S.; Civil, W.; Lapworth, D.J.; MacDonald, A.M.; McKenzie, A.A.; Read, D.S.; Sekhar, M.; Singer, A.C.; Thankachan, A.; et al. Presence of emerging organic contaminants and microbial indicators in surface water and groundwater in urban India. *Environ. Pollut.* **2024**, *362*, 124983. [CrossRef]
27. Dikobe, P.I.; Tekere, M.; Masindi, V.; Foteinis, S. Occurrence, persistence, and removal of contaminants of emerging concern through drinking water treatment processes—A case study in South Africa. *Environ. Nanotechnol. Monit. Manag.* **2024**, *22*, 100997. [CrossRef]
28. Wishart, D.S.; Feunang, Y.D.; Guo, A.C.; Lo, E.J.; Marcu, A.; Grant, J.R.; Sajed, T.; Johnson, D.; Li, C.; Sayeeda, Z.; et al. DrugBank 5.0: A major update to the DrugBank database for 2018. *Nucleic Acids Res.* **2017**, *46*, D1074–D1082. [CrossRef] [PubMed]
29. Sigurnjak, M.; Ukić, Š.; Cvetnić, M.; Markić, M.; Novak Stankov, M.; Rasulev, B.; Kušić, H.; Lončarić Božić, A.; Rogošić, M.; Bolanča, T. Combined toxicities of binary mixtures of alachlor, chlorfenvinphos, diuron and isoproturon. *Chemosphere* **2020**, *240*, 124973. [CrossRef]
30. Loewe, S.; Muischnek, H. Über kombinationswirkungen. 1. Mitteilung: Hilfsmittel der Fragestellung. *N.-S. Arch. Ex. Path* **1926**, *114*, 313–326. [CrossRef]
31. Loewe, S. Die Mischarznei. Versuch einer allgemeinen Pharmakologie der Arzneikombinationen. *Kline Wochenschr.* **1927**, *6*, 1077–1085. [CrossRef]
32. Schell, T.; Goedkoop, W.; Zubrod, J.P.; Feckler, A.; Lüderwald, S.; Schulz, R.; Bundschuh, M. Assessing the effects of field-relevant pesticide mixtures for their compliance with the concentration addition model—An experimental approach with *Daphnia magna*. *Sci. Total Environ.* **2018**, *644*, 342–349. [CrossRef]
33. Qin, L.-T.; Liu, S.-S.; Zhang, J.; Xiao, Q.-F. A novel model integrated concentration addition with independent action for the prediction of toxicity of multi-component mixture. *Toxicology* **2011**, *280*, 164–172. [CrossRef] [PubMed]
34. Puckowski, A.; Stolte, S.; Wagil, M.; Markiewicz, M.; Łukaszewicz, P.; Stepnowski, P.; Białk-Bielińska, A. Mixture toxicity of flubendazole and fenbendazole to *Daphnia magna*. *Int. J. Hyg. Environ. Health* **2017**, *220*, 575–582. [CrossRef]
35. Backhaus, T.; Faust, M. Predictive environmental risk assessment of chemical mixtures: A conceptual framework. *Environ. Sci. Technol.* **2012**, *46*, 2564–2573. [CrossRef] [PubMed]
36. Bliss, C.I. The toxicity of poisons applied jointly. *Ann. Appl. Biol.* **1939**, *26*, 585–615. [CrossRef]
37. *ISO 11348-1:2007*; Water Quality—Determination of the Inhibitory Effect of Water Samples on the Light Emission of *Vibrio fischeri* (Luminescent Bacteria Test). Part 1: Method Using Freshly Prepared Bacteria. International Organization for Standardization: Geneva, Switzerland, 2007.
38. Abbas, M.; Adil, M.; Ehtisham-ul-Haque, S.; Munir, B.; Yameen, M.; Ghaffar, A.; Shar, H.A.; Tahir, M.A.; Iqbal, M. *Vibrio fischeri* bioluminescence inhibition assay for ecotoxicity assessment: A review. *Sci. Total Environ.* **2018**, *626*, 1295–1309. [CrossRef] [PubMed]
39. Kumar, A.; Podder, T.; Kumar, V.; Kumar Ojha, P. Risk assessment of aromatic organic chemicals to T. pyriformis in environmental protection using regression-based QSTR and Read-Across algorithm. *Process Saf. Environ. Prot.* **2023**, *170*, 842–854. [CrossRef]
40. Han, Z.; Cong, P.; Qiu, J. Microscopic experimental and numerical research on rejuvenators: A review. *J. Traffic Transp. Eng.* **2022**, *9*, 180–207. [CrossRef]
41. Kashyap, D.K.; Kushwaha, N.D.; Gupta, J.; Verma, K.K.; Srivastav, M. Innate synthesis of 1,3-oxathiolan-5-one derivatives & its antimicrobial potential. *J. Chem. Pharm. Res.* **2015**, *7*, 108–113.
42. Available online: https://pubchem.ncbi.nlm.nih.gov/compound/Oseltamivir (accessed on 20 September 2024).
43. Mallhi, T.H.; Butt, M.H.; Ahmad, A.; Misbah, S.; Salman, M.; Khan, A.; Raja, A.A.; Khan, Y.H. Chapter 5—Drug-metabolizing enzymes and fate of prodrugs: From function to regulation. In *Biochemistry of Drug Metabolizing Enzymes*; Akash, M.S.H., Rehman, K., Eds.; Academic Press: San Diego, CA, USA, 2022; pp. 125–139. [CrossRef]
44. Escher, B.I.; Bramaz, N.; Lienert, J.; Neuwoehner, J.; Straub, J.O. Mixture toxicity of the antiviral drug Tamiflu® (oseltamivir ethylester) and its active metabolite oseltamivir acid. *Aquat. Toxicol.* **2010**, *96*, 194–202. [CrossRef] [PubMed]
45. van Beek, S.J. Treatment of Antiviral Drugs in Wastewater Using Advanced Oxidation Processes—Ozonation of Oseltamivir Phosphate. Master's Thesis, University of Alberta, Edmonton, AB, Canada, 2021.
46. Huang, T.; Jiang, H.; Zhao, Y.; He, J.; Cheng, H.; Martyniuk, C.J. A comprehensive review of 1,2,4-triazole fungicide toxicity in zebrafish (*Danio rerio*): A mitochondrial and metabolic perspective. *Sci. Total Environ.* **2022**, *809*, 151177. [CrossRef] [PubMed]
47. Dong, Y.; Fang, Z.; Xu, Y.; Wang, Q.; Zou, X. The toxic effects of three active pharmaceutical ingredients (APIs) with different efficacy to *Vibrio fischeri*. *Emerg. Contam.* **2019**, *5*, 297–302. [CrossRef]
48. Guo, Z.; He, H.; Liu, K.; Li, Z.; Yang, S.; Liao, Z.; Lai, C.; Ren, X.; Huang, B.; Pan, X. The photolytic behavior of COVID-19 antivirals ribavirin in natural waters and the increased environmental risk. *J. Hazard. Mater.* **2023**, *452*, 31320. [CrossRef]
49. Kalyaev, M.V.; Ryabukhin, D.S.; Borisova, M.A.; Ivanov, A.Y.; Boyarskaya, I.A.; Borovkova, K.E.; Nikiforova, L.R.; Salmova, J.V.; Ul'yanovskii, N.V.; Kosyakov, D.S.; et al. Synthesis of 3-Aryl-3-(Furan-2-yl)Propanoic Acid Derivatives, and Study of Their Antimicrobial Activity. *Molecules* **2022**, *27*, 4612. [CrossRef]

50. March, R.B.; Georghiou, G.P.; Metcalf, R.L.; Printy, G.E. The comparative toxicity of phosphoramidothionates and phosphoramidates to susceptible and insecticide-resistant houseflies and mosquitos. *Bull. World Health Organ.* **1964**, *30*, 71–84. [PubMed]
51. Farrell, R.E.; Steele, H.; Middleton, R.J.; Skropeta, D.; Liu, G.-J. Cytotoxicity of phosphoramidate, bis-amidate and cycloSal prodrug metabolites against tumour and normal cells. *RSC Med. Chem.* **2024**, *15*, 1973–1981. [CrossRef] [PubMed]
52. Mohankumar, A.; Ranjitha, P. Purification and characterization of esterase from marine *Vibrio fischeri* isolated from squid. *Indian J. Mar. Sci.* **2010**, *39*, 262–269.
53. Snider, J.D. Characterization of the MoxR Family of AAA+ ATPases. Ph.D. Thesis, University of Toronto, Toronto, ON, Canada, 2007.
54. Parvez, S.; Venkataraman, C.; Mukherji, S. Toxicity assessment of organic pollutants: Reliability of bioluminescence inhibition assay and univariate QSAR models using freshly prepared *Vibrio fischeri*. *Toxicol. In Vitro* **2008**, *22*, 1806–1813. [CrossRef]
55. Wang, X.H.; Fan, L.Y.; Wang, S.; Wang, Y.; Yan, L.C.; Zheng, S.S.; Martyniuk, C.J.; Zhao, Y.H. Relationship between acute and chronic toxicity for prevalent organic pollutants in *Vibrio fischeri* based upon chemical mode of action. *J. Hazard. Mater.* **2017**, *338*, 458–465. [CrossRef]
56. Tetko, I.V.; Gasteiger, J.; Todeschini, R.; Mauri, A.; Livingstone, D.; Ertl, P.; Palyulin, V.A.; Radchenko, E.V.; Zefirov, N.S.; Makarenko, A.S.; et al. Virtual computational chemistry laboratory—Design and description. *J. Comput. Aid. Mol. Des.* **2005**, *19*, 453–463. [CrossRef] [PubMed]
57. Cumming, F.; Rücker, C. Octanol−Water Partition Coefficient Measurement by a Simple ^{1}H NMR Method. *ACS Omega* **2017**, *2*, 6244–6249. [CrossRef] [PubMed]
58. Moldoveanu, S.; David, V. Chapter 5—Phase transfer in sample preparation. In *Modern Sample Preparation for Chromatography*, 2nd ed.; Moldoveanu, S., David, V., Eds.; Elsevier: Oxford, UK, 2021; pp. 151–190. [CrossRef]
59. Alberts, B.; Johnson, A.; Lewis, J.; Raff, M.; Roberts, K.; Walter, P. *Molecular Biology of the Cell*, 5th ed.; Garland Science: New York, NY, USA, 2007; pp. 617–629.
60. Bobrowski, T.; Chen, L.; Eastman, R.T.; Itkin, Z.; Shinn, P.; Chen, C.Z.; Guo, H.; Zheng, W.; Michael, S.; Simeonov, A.; et al. Synergistic and Antagonistic Drug Combinations against SARS-CoV-2. *Mol. Ther.* **2021**, *29*, 873–885. [CrossRef] [PubMed]